

Effect of particle presence on gas phase temperature in the flame spray pyrolysis

Sascha R. Engel^{1,2}, Yi Gao^{1,2}, Andreas F. Koegler¹, Daniel Kilian³, Thomas Seeger^{2,4}, Wolfgang Peukert³ and Alfred Leipertz^{1,2}

¹Institute of Engineering Thermodynamics, University of Erlangen-Nuremberg, Erlangen, Bavaria, 91058, Germany

²Erlangen Graduate School in Advanced Optical Technologies, University of Erlangen-Nuremberg, Erlangen, Bavaria, 91052, Germany

³Institute of Particle Technology, University of Erlangen-Nuremberg, Erlangen, Bavaria, 91058, Germany

⁴Institute of Engineering Thermodynamics, University of Siegen, Siegen, North Rhine-Westphalia, 57072, Germany

ABSTRACT

For the production of manufactured nanoparticles at a commercial scale flame processes are most frequently used. An important basis for understanding the complexity of this process is the characterization of the combustion process in dependence of the operation conditions. As minor changes of process parameters have huge impact on the product, invasive classic methods would fail. Hence, there is a demand for non-invasive advanced optical measurement tools acquiring data regarding the flame and the particle formation without changing the product by the applied measuring technique. In this work, gas phase temperatures, significantly influencing product particle sizes, were acquired by O₂-based pure rotational CARS during flame spray pyrolysis (FSP) and were compared for a particle-free and a particle-laden flame. Furthermore, the influence of different precursor concentrations on the distribution of the liquid regime was investigated by Mie scattering.

Keywords: Flame spray pyrolysis, rotational CARS, temperature measurement, spray combustion, nanoparticles

1 FLAME SPRAY PYROLYSIS (FSP)

Figure 1 shows a schematic diagram of the **FSP process**. The burner design is annular. The precursor hexamethyldisiloxane (HMDSO) and its organic solvent (EtOH) are injected for silica production through a capillary tube placed in the center of the burner. The precursor feed is dispersed with oxygen. The methane/oxygen support flame is used to ignite and sustain the spray combustion. An oxygen sheath gas flowing through a sintered metal ring placed around the annular gap of the support flame stabilizes and shields the spray flame. Geometrical details and a further description of the burner can be found elsewhere [1]. For a HMDSO precursor concentration of 0.5 mol·l⁻¹ a primary particle size of 8.2 nm was measured using nitrogen gas adsorption. The particle size was determined by the evaluation of the nitrogen gas adsorption data with the BET model [2].

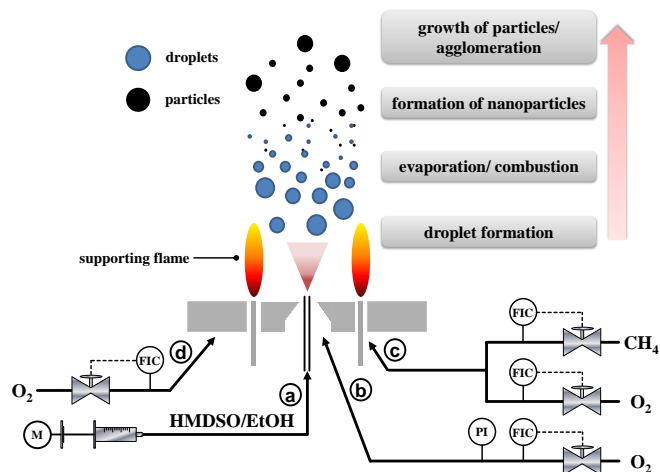


Figure 1: Schematic diagram of the flame spray pyrolysis process; a: precursor in organic solvent, HMDSO/EtOH (5 ml·l⁻¹); b: dispersion gas, oxygen (5 sl·min⁻¹); c: inlet support flame gases, premixed methane (1.5 sl·min⁻¹) and oxygen (5 sl·min⁻¹); d: sheath gas, oxygen (10 sl·min⁻¹)

2 TEMPERATURE MEASUREMENTS

2.1 Experimental setup rotational CARS

Gas phase temperatures were measured in a pure oxygen flame spray pyrolysis process by O₂-based pure rotational CARS applying a polarization technique essential to acquire nearly undisturbed CARS spectra in particle and droplet environments good enough to qualify for quantitative data evaluation. The **CARS system** shown in Fig. 2 is based on a multimode frequency-doubled 30 Hz Nd:YAG laser system (Spectra Physics, PRO 250-30) with a pulse energy of 500 mJ at 532 nm. 90 % of the energy was split off to pump a broadband dye laser (DCM). The dual-broadband rotational CARS signal was generated by two broadband dye laser beams and one frequency-doubled Nd:YAG laser beam. The DCM dye, centered around 630 nm with a width of 500 cm⁻¹, produced approximately 25 mJ per pulse. In order to obtain high spatial resolution in the point measurements, a planar BOXCARS configuration with a focusing lens of $f = 300$ mm was used. The CARS

signal was dispersed by a 0.5-m spectrograph (Triax 550) equipped with a 2400 g/mm grating and recorded by a CCD camera (PCO 2000).

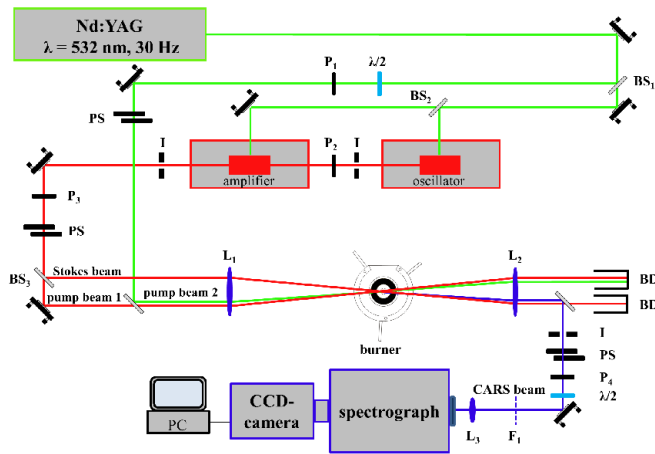


Figure 2: Experimental setup for O_2 -based pure rotational CARS measurements with polarization filtering. BS₁: T90/R10; BS₂: T80/R20; BS₃: T65/R35 (BS: beam splitter with transmission T and reflection R); L₁₋₃: spherical lenses; F₁: long-pass Razor Edge (laser line 532 nm); P₁₋₄: polarizers; PS: periscope; I: iris; BD: beam dump; the blue shifted CARS signal is indicated by the blue color of the CARS signal path in the diagram

The application of CARS in a reacting multi-phase environment characterized by droplets, particles and huge density gradients requires the suppression of non-resonant background and scattered light by a certain **polarization filtering technique**. The angles at which the resonant and nonresonant signals were emitted ($\beta = -26.6^\circ$ and $\delta = 18.4^\circ$), are calculated, e.g., according to Leipertz and Seeger [3]. The maximum resonant signal was detected at 45° , which is the polarization angle between the probe and the pump beam and therefore defines the coordinate origin. The polarization angle between the polarizations of the pump beam and Stokes beam was set to 0° . By this way, the Nd:YAG laser polarization was set perpendicular to the analyzer in the signal path to suppress parts of the elastically scattered stray light. This arrangement results in a theoretical resonant signal loss approximately of a factor of 1.8. This technique greatly reduced the stray light but was not sufficient for the spray experiments. Therefore, remaining elastic stray light was completely removed by a knife-edge, placed on the camera window, filtering low Raman shifts [4]. A second problem is the unknown varying nonresonant signal contribution depending on the local gas temperature [5]. This is reduced approximately by a factor of 5 due to the polarization arrangement described. Further details of the CARS setup and data processing are described in detail elsewhere [6]

2.2 Sort out procedure for CARS spectra

Essential for temperature evaluation in the harsh environment of a spray flame is the careful **selection of the**

acquired CARS spectra. In this regards, CARS spectra comprising of two superimposed envelopes due to temperature gradients in the measurement volume were identified and sorted out manually. These spectra could be easily recognized because they result for the FSP-flame in a bimodal rotational CARS spectrum as shown in Fig. 3 as a dashed black line. Additionally, spectra indicating laser-induced breakdowns from droplets or particles as shown in Fig. 3 as a solid red line were also sorted out. The probability of breakdowns strongly depends on the measurement location. A spectrum suitable for temperature fitting is displayed as a dotted blue line in Fig. 3. Approximately 80 % of the recorded spectra within the particle respectively droplet regime were sorted out due to temperature gradients and breakdowns in the measurement volume, and only 20 % could be used for temperature calculation.

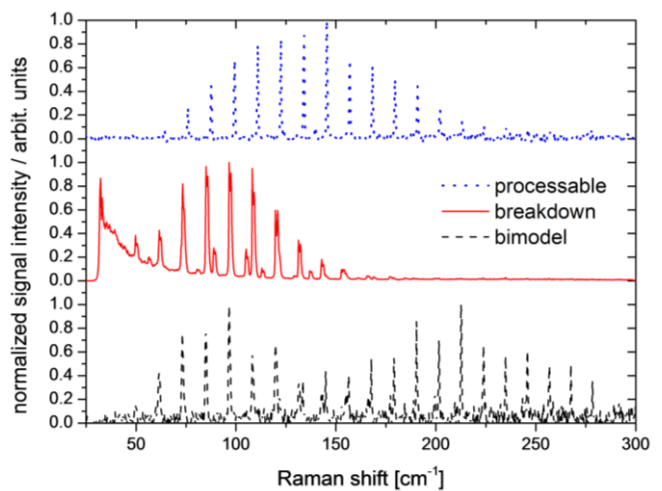


Figure 3: The diagram shows a bimodal CARS spectrum (dashed black), a breakdown affected CARS spectrum (solid red) and a CARS spectrum suitable for temperature fitting (dotted blue)

2.3 Influence of particles on gas phase temperature

Gas phase temperatures acquired by O_2 -based pure rotational CARS results are illustrated in Fig. 4. Here, the gas phase temperature recorded 2 mm away from the nozzle is plotted over the height above burner. The burner was operated with pure ethanol (\square) and HMDSO at a concentration of $0.5 \text{ mol}\cdot\text{l}^{-1}$ (\diamond). Black arrows indicate the measured temperature differences for the particle-free (\square) and the particle-laden (\diamond) spray flame. Measured temperatures in regimes carrying particles in a particle producing flame, are significantly higher for particle-free than for particle-laden flames. This indicates the **dissipation of energy by radiation in the presence of particles**.

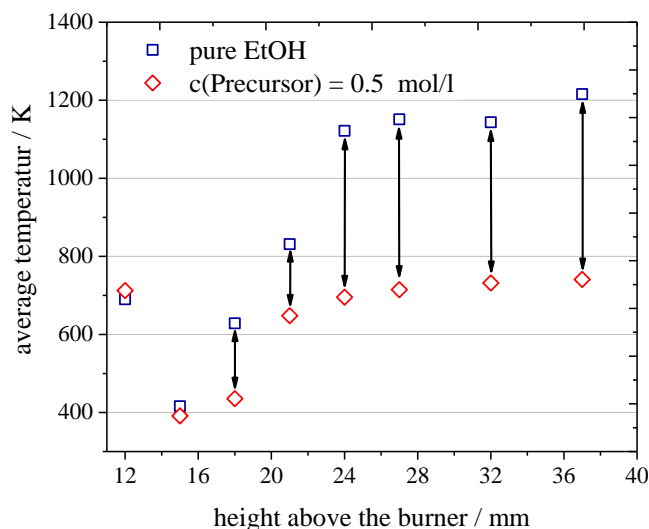


Figure 4: Axial temperature profiles with a radial distance of 2 mm from the nozzle obtained with pure rotational CARS. The liquid feed was pure ethanol (\square) and HMDSO in ethanol with a concentration of $0.5 \text{ mol}\cdot\text{l}^{-1}$ (\diamond). Temperatures are based on 500 recorded single-shot CARS spectra

2.4 Temperature gradients quantified in single-shot CARS measurements

The probe volume of the CARS measurements, defined by the overlap of the focussed Stokes, pump and probe beam, had a diameter of $\sim 100 \mu\text{m}$ and a length of $\sim 2 \text{ mm}$. A sanity-check proved that the probe volume is sufficiently small to resolve the dimension of the flame. The probe volume was measured by translating a glass cover slip through the beam crossing region and monitoring the rotational CARS signal. A summation of the accumulated CARS intensities along the beam propagation axis produces a sum curve. The 5% and 95% values of the maximum integrated intensity are applied to the sum curve to determine a length of $\sim 2 \text{ mm}$ for the probe volume [7].

Fig. 5 shows a CARS spectra comprised of two temperature envelopes fitting to a cold gas phase temperature of 350 K and a hot temperature of 2550 K. Therefore, a **temperature gradient** of 2200 K could be resolved within this 2 mm and a single-shot measurement with a temporal resolution equal to the pulse duration of the laser (6–10 ns). The measuring location indicated by a white dot in an average OH chemiluminescence image on the left side resides in the interface of the spray and the surrounding flame. Distinct temperature gradients are characteristic of flame spray pyrolysis due to interfaces generated by the dense annular alignment of the gas and liquid outlets illustrated by Fig. 1.

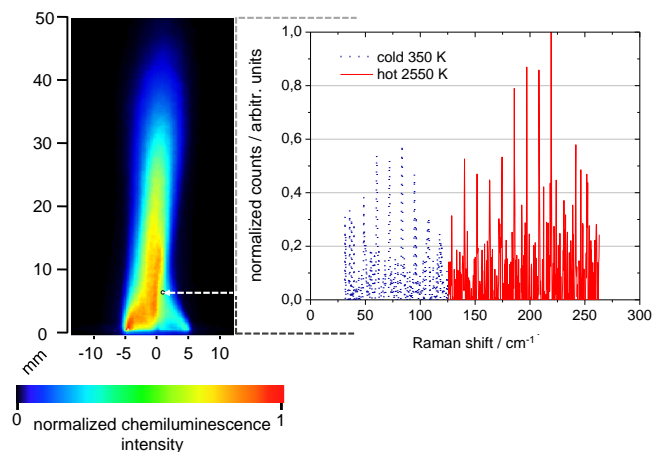


Figure 5: Temperature gradient acquired in a single-shot pure rotational CARS measurement. The point of measurement, 6 mm above the burner and 1 mm right from the center, is indicated by a white dot in the chemiluminescence image. The propagation of the laser beam is perpendicular to the image plane. Silica nanoparticles were produced with HMDSO as precursor. Left: normalized and averaged ($n = 500$) OH chemiluminescence image of the particle-laden flame; right: single-shot CARS spectrum divided in hot and cold part.

3 DROPLET DISTRIBUTION MEASUREMENTS

3.1 Experimental setup Mie scattering

Mie scattering experiments were carried out to visualize the droplet distribution for different precursor concentrations. A schematic of the **Mie scattering setup** is displayed in Fig. 6. Mie scattering was excited with a Nd:YAG laser (Quantel, Big Sky) at 532 nm with a repetition rate of 10 Hz and a pulse duration of 8 ns. The pulse energy per pulse was set to 28 mJ. The laser light sheet (thickness $\sim 200 \mu\text{m}$), formed by a telescope system composed of an expanding lens $f = -100$, a collimating lens $f = 250$ and a cylindrical lens $f = 750$ placed in front of the burner, interacts with the droplets in the spray combustion. Mie scattering from the laser light sheet plane was captured at 90° from the incident light using a 12 bit charged-coupled device (CCD) camera (LaVision, E-Lite 1.4M). The resolution of the CCD chip is 1392×1040 pixels with a pixel size of $6.45 \times 6.45 \mu\text{m}^2$. A 105-mm UV Nikkor F/4.5 lens was employed with one 14-mm extension ring to collect Mie scattering emissions. $90 \mu\text{m}$ could be mapped on one pixel of the CCD chip which corresponds with a magnification factor of 0.07. Two neutral density filters with OD 0.5 and OD 0.6 in front of lens prevented oversaturation of the camera chip. Camera acquisition and laser emission was synchronized by a pulse delay generator.

4 CONCLUSION

The CARS results in the particle regime show significantly decreasing flame temperatures in the presence of particles since energy is dissipated rapidly by radiation heat transfer. Mie scattering results display unchanged droplet distributions for varying precursor concentrations. Therefore, measured temperature differences can be exclusively attributed to the presence of particles. Additionally, temperature gradients of 2200 K were resolved within the probe volume of 0.1×2 mm (diameter \times length) and a temporal resolution of a single laser shot (6 – 10 ns).

5 REFERENCES

1. L. Mädler, H. K. Kammler, R. Mueller, and S. E. Pratsinis, "Controlled synthesis of nanostructured particles by flame spray pyrolysis," *J. Aerosol Sci.* **33**, 369-389 (2002).
2. S. Brunauer, P. Emmett, and E. Teller, "Adsorption of gases in multilayers," *J. Am. Chem. Soc.* **60**, 309-319 (1938).
3. A. Leipertz and T. Seeger, "Combustion diagnostics by pure rotational coherent anti-Stokes Raman scattering," in *Optical processes in microparticles and nanostructures : a festschrift dedicated to Richard Kounai Chang on his retirement from Yale University* (World Scientific Pub., Singapore; Hackensack, NJ, 2011).
4. F. Beyrau, A. Bräuer, T. Seeger, and A. Leipertz, "Gas-phase temperature measurement in the vaporizing spray of a gasoline direct-injection injector by use of pure rotational coherent anti-Stokes Raman scattering," *Opt. Lett.* **29**, 247-249 (2004).
5. F. Vestin, M. Afzelius, and P.-E. Bengtsson, "Development of rotational CARS for combustion diagnostics using a polarization approach," *Proc. Combust. Inst.* **31**, 833-840 (2007).
6. T. Seeger, F. Beyrau, A. Braeuer, and A. Leipertz, "High pressure pure rotational CARS: Comparison of temperature measurements with O_2 , N_2 , and synthetic air," *J. Raman Spectrosc.* **34**, 932 - 939 (2003).
7. S. A. Tedder, M. C. Weikl, T. Seeger, and A. Leipertz, "Determination of probe volume dimensions in coherent measurement techniques," *Appl. Opt.* **47**, 6601-6605 (2008).

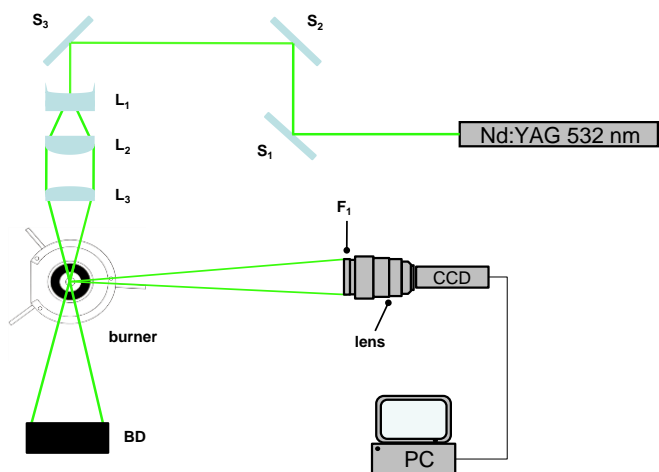


Figure 6: Experimental setup for Mie imaging measurements. L_1 : spherical lens $f = -100$ mm; L_2 : spherical lens $f = 250$ mm; L_3 : cylindrical lens $f = 750$ mm; $S_1 - S_3$: mirrors, highly reflective for light at 532 nm; F_1 : ND with OD 0.5 and 0.6; BD: beam dump.

3.2 Droplet distribution for different precursor concentrations

Figure 7 shows the axial distribution of the Mie scattering intensity for different precursor concentrations. The location of the axial line profile in the spray flame is indicated by a white solid line in the average Mie scattering image on the upper right side. The **Mie scattering experiments show no significant change in the droplet distribution for different HMDSO precursor concentrations** ranging from 0 to $1 \text{ mol}\cdot\text{l}^{-1}$. This demonstrates that different precursor concentrations typical for the flame spray pyrolysis process have no significant influence on the spray evaporation process.

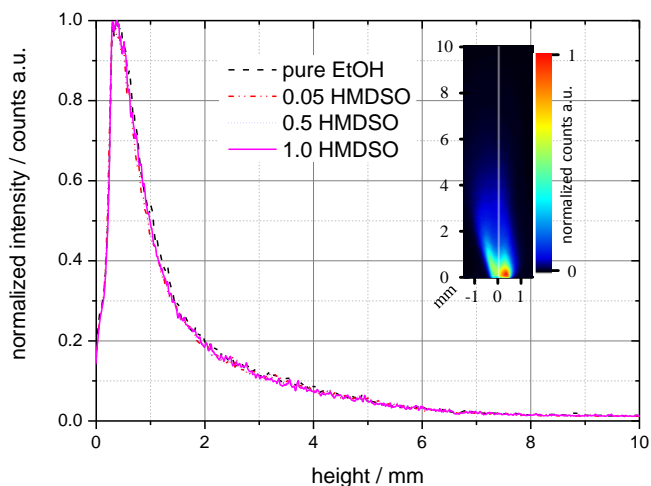


Figure 7: Axial distribution of the Mie scattering intensity for different precursor concentrations of 0, 0.05, 0.5 and $1.0 \text{ mol}\cdot\text{l}^{-1}$ HMDSO in ethanol centered above the nozzle exit. The averaged Mie scattering image plotted on the upper right side within the diagram is based on 500 single-shot images. The solid white line in the image indicates the position of the axial line plot